	あ　か　さい　けん
氏　　　　　　名	阿　加　賽　見
研究科，専攻の名称	東北大学大学院工学研究科（博士課程）ナノメカニクス専攻
学 位 論 文 題 目	Study of Nano-Scale Flattening Mechanisms of Metal Surfaces by a Photoemission-assisted Plasma Ion Source（光電子制御プラズマイオン源による金属表面のナノスケール平坦化機構に関する研究）
論 文 審 査 委 員	主査　東北大学教授　高桑　雄二　東北大学教授　羽根　一博 　　　東北大学教授　足立　幸志　東北大学教授　虻川　司

論文内容要約

Clean and flattened surfaces play an important role in the surface activated bonding (SAB). The crucial surface roughness for Cu-Cu SAB process at room temperature have been reported as < 2 nm. As the conventional process of the surface treatment, the chemical mechanical polishing/planarization (CMP) has been used, which cannot meet the challenge of the defect free and clean surface demanded in the SAB due to the wet process. Besides the defects and damages induced by CMP, thick oxide layer could be induced on the surfaces. On the other hand, as a dry process, the fast atom beam (FAB) and conventional ion beam irradiation commonly induce the undesirable roughened and nanostructured surfaces for SAB process. Furthermore, the low energy gas cluster ion beam irradiation can demonstrate an excellent flat surface down to sub-nanometer but with removal of around 100 nm of the materials. Besides the sputtering off the amount of the materials, the processed area of surface by GCIB is reported as small as 1×1 cm^2, which is considered not suitable for wafer-sized thin film surface flattening.

This study aims to develop a dry process for atomic-level flattening of metal surfaces by using photoemission-assisted plasma (PAP) ion source with low ion kinetic energy (E_{ion}) and capable for large area surface processing. The PAP is based on the direct current discharge and triggered by photoelectrons emitted from the cathode substrate surface as shown in Fig. 1. Since the substrate is set on the cathode side, positive gas ions such as Ar^+ ions can irradiate to the substrate. As the result, the surface flattening of the substrate is expectable by the ion irradiation. In this context, this study is motivated by three questions: (1) How is the generation mechanism and E_{ion} of PAP? (2) How does the Cu surface morphology change after PAP irradiation? (3) Could the wafer-sized surfaces be flattened after PAP irradiation?

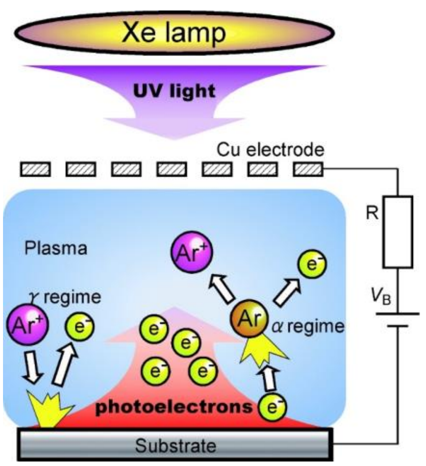

Fig. 1. Schematic diagram of photoemission-assisted plasma ion source used for surface flattening.

To illustrate these questions, in chapter 2, firstly, the discharge characteristics measurements of the PAP ion source were conducted. Secondly, based on the plasma potential measured by Langmuir probe method, the E_{ion} of the Ar^+ ions were evaluated. Finally, to verify the reliability of the evaluated E_{ion}, the sputtering yield (Y_s) of Ar^+ ion on Cu surface was experimentally performed and compared with the other reported data. In chapter 3, Cu surfaces were irradiated by Ar^+ ion generated by PAP with E_{ion} near and below the threshold energy of physical sputtering (E_{th}: ~ 25 eV) to show how the morphology of Cu surface changes after low energy ion irradiation. In chapter 4, based on the work function (WF) measurements of the Cu surface observed by ultraviolet photoelectron microscopy (UPS) after ion irradiation, the mechanism of low energy ion interaction with the Cu surface was constructed. In chapter 5, 3-inch sized Cu surface was flattened by PAP Xe^+ ion irradiation based on the understanding of the momentum transfer effect on the morphological changes of Cu surface by comparing the low E_{ion} Xe^+ and Ar^+ ion irradiation.

In chapter 2, based on the discharge characteristics, it was clarified that the breakdown voltage of PAP can be decreased owing to the existence of photoelectrons, which could contribute to lower down the E_{ion} compared with the normal DC discharge plasma. The plasma potential (V_s) along the discharge distance (d) was measured using Langmuir probe method, demonstrating that there is an ion sheath formed near the substrate surface. Thus, the ions can be accelerated by the potential driven on the sheath area. The electric potential distribution draws a parabola toward substrate surface, consequently, the electric field in the sheath area is a linear function of the distance, and it has the maximum value at substrate surface as $2V_s/d_s$, where d_s is the sheath width. Consideration of the high-gas pressure condition in PAP ion source, the ions are not only accelerated by the electric field through the sheath, but also decelerated by the collisions between ions and neutrals when the ions cross over the sheath area to the substrate surface. The evaluation of E_{ion} uses the charge transfer collision of ion and its neutral atoms when ion crosses though the collisional matric sheath. As a result, the E_{ion} was evaluated changeable from 0.1 ~ 300 eV by adjusting the gas pressure and bias voltage of PAP as shown in Fig. 2. The estimation of Y_s of Ar^+ ion on the Cu surface was carried out and demonstrated a good agreement of the experimental results by others. It was decreased down to ~ 10^{-3} atoms/ion at E_{ion} < 50 eV, suggesting that the Y_s can be decreased down to ~ 10^{-4} atoms/ion when the E_{ion} lower than E_{th}.

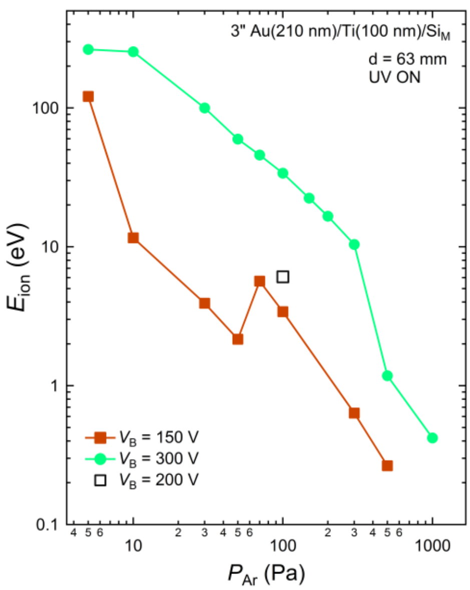

Fig. 2 Dependence of E_{ion} on Ar gas pressure. V_B is the bias voltage applied between the electrode and the Cu substrate surface.

In chapter 3, the morphological changes of Cu surfaces by Ar^+ ion irradiation have been investigated. The findings based on the AFM images and corresponding analysis of surface roughness, surface height distribution and power spectral density (PSD) showed that using E_{ion} = 10.5 eV (near E_{th} of Ar^+ ion on Cu: 17 eV) ion irradiation, it can induce pronounced surface structures as protrusions, resulting a rough surface. The protrusion formation was considered as a coupling effect of sputtering, redeposition and surface migration. The redeposition was contributed by combination of the thermalization and ballistic diffusion of the sputtered Cu atoms. The surface migration was mainly induced by the collision motivated diffusion. Moreover, in comparison, FAB with beam energy of 1.45 keV irradiated on Cu/Si surfaces, showing Cu thin film on the Si substrate were sputtered off and the surface of the Si substrate was visible due to higher energy Ar^0-FAB sputtering. On the other hand, using E_{ion} = 1.1 eV ion irradiation as shown in Fig. 3(a)-(b), the root mean square surface roughness (R_q) of the Cu surface decreased about 40% comparison to the initial surface with increasing irradiation charge (Q = I_D×t, I_D is the discharge current) up to 1.74 C. The results suggested that the enhancement of surface migration induced by collision motivated diffusion takes account for the flattening of Cu surfaces. Moreover, I_D during irradiation showed a dip-like structure at the initial stage, which is considered related to the surface oxide reduction/removal.

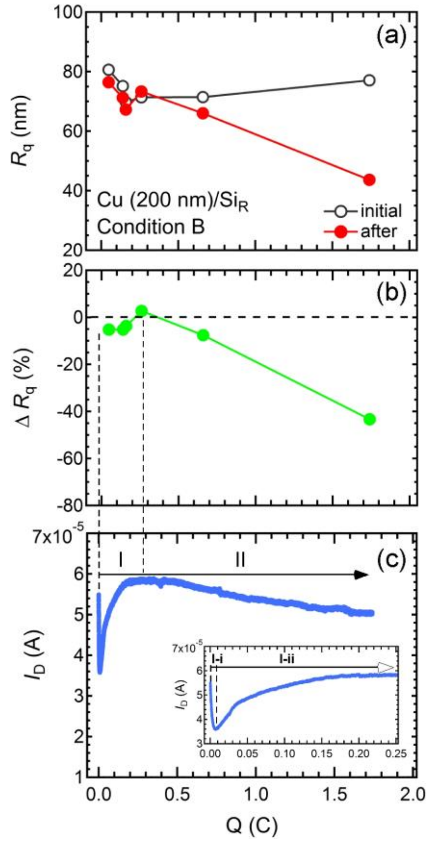

Fig. 3. Dependence of Q on (a) R_q (b) △ R_q, and (c) I_D-Q curve during Ar^+ ion irradiation with E_{ion} = 1.1 eV.

In chapter 4, the WF of the Cu surface were observed by UPS during ion irradiation. Consideration of the trend of the I_D and the WF, it is understood that there was an incubation time for the surface oxide removal as shown in Fig. 4(a)-(d). After reduction/removal of the surface oxide, the Cu atoms can receive kinetic energy and momentum from the incoming ion and diffusion along the surface for flattening. Moreover, it was confirmed that the surface oxide can be reduced by the UV light irradiation, which is emitted from the Xe excimer lamp with photoenergy about 7.2 eV.

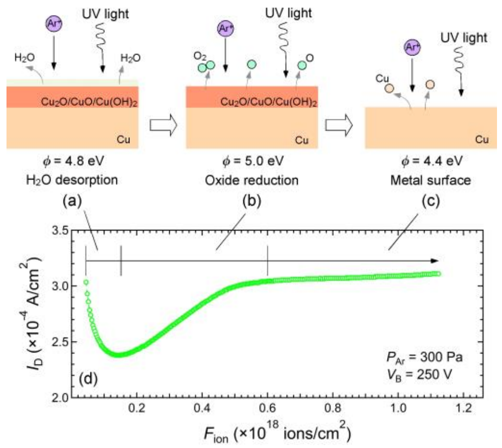

Fig. 4. Models of (a) the initial Cu surface covered with native oxide and hydrooxide, irradiating by Ar^+ ion, (b) removal of surface oxide by Ar^+ ion and UV light irradiation, (c) apperance of clean surface. (d) I_D-F_{ion} curve during ion irradiation on Cu surface.

In chapter 5, the surface morphological changes of the Cu surfaces were investigated with Ar^+-PAP, and Xe^+-PAP irradiation at E_{ion} = 26 eV, respectively. By Ar^+-PAP irradiation, surface roughness increased from 2.25 to 5.36 nm due to crater formation. In contrast, Cu surface was flattened by Xe^+-PAP with decreasing R_q from 2.91 to 1.29 nm. The difference of the Cu surface morphological changes induced by Xe^+ than Ar^+ ion irradiation was due to the difference of the Y_s and adatom yield. The Y_s were measured as 2.84×10^{-3} and 5.61×10^{-3} atoms/ion for Xe^+ and Ar^+ ion irradiation on the Cu surfaces at E_{ion} = 26 eV. The flattening effect was contributed by relatively low sputtering yield and high adatom yield of Xe^+ than that of Ar^+ ion irradiation on the Cu surface. Higher adatom yield suggested the higher rate of the adatom migration, which was enhanced by collision motivated diffusion with Xe^+ ion irradiation.

In this context, 3-inch sized Cu surfaces were irradiated by Xe^+-PAP E_{ion} = 26 eV, demonstrating a significant decrease in R_q. As shown in Fig. 5(a), the R_q was measured along the distance from the sample edge. R_q of the 3-inch Cu surface decreased from 4.14 to 1.95 nm after PAP Xe^+ ion irradiation as shown in Fig. 5(b), which met the critical roughness condition for SAB process. Moreover, it is reported that the surface smoothing rate slows down for higher ion fluence due to the surface initial cone like structures smoothed out, and the surface depressions have a relatively lower erosion rate. As shown in Fig. 5(c) that the slop of the R_q dependence of ion fluence was constant revealing further surface flattening effect could be obtained by increasing ion fluence of Xe^+ ion. Although the 3-inch substrate was decreased from 4.14 to ~ 1.95 nm, more reduction of roughness can be expectable after optimizing the PAP discharge conditions such as E_{ion}, ion flux and ion fluence.

The PAP ion source exhibited the potential applications not only in the field of wafer bonding, but also in the thin film growth by chemical vapor deposition process using PAP ion source.

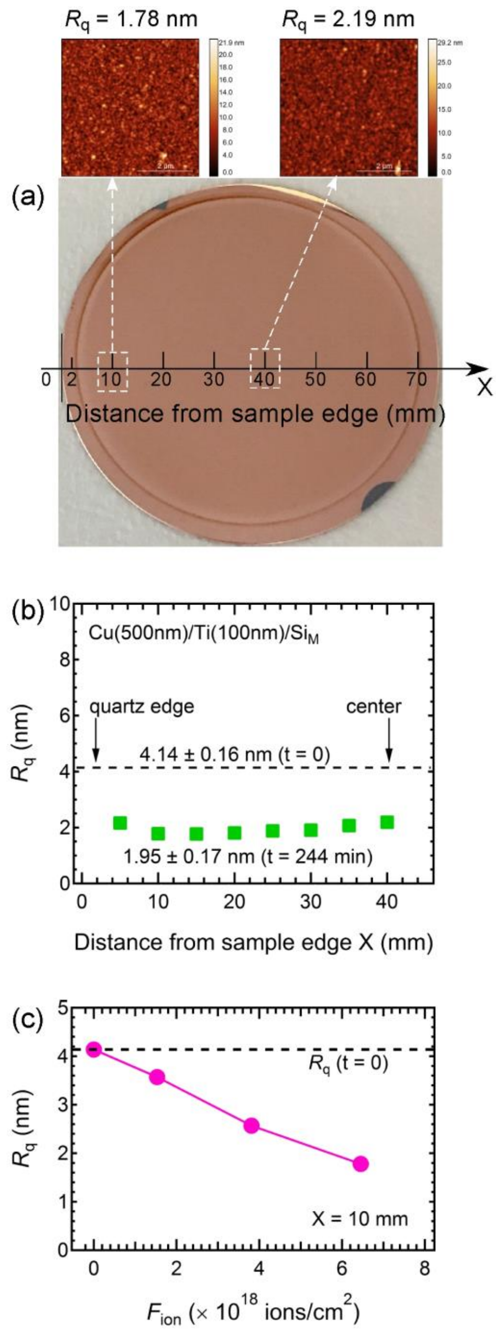

Fig. 5. (a) Picture of a 3-inch sized Cu substrate after 26-eV Xe^+-PAP irradiation, and corresponding AFM images at X = 10, 40 mm, (b) the evolution of R_q with distance from the sample edge, ion fluence was 6.45×10^{18} ions/cm^2. (c) dependence of R_q on ion fluence.